A peer-reviewed version of this preprint was published in PeerJ on 1 November 2019.

View the peer-reviewed version (peerj.com/articles/7956), which is the preferred citable publication unless you specifically need to cite this preprint.

Lazcano-Hernández H, Aguilar G, Dzul-Cetz GA, Patiño R, Arellano-Verdejo J. 2019. Off-line and on-line optical monitoring of microalgal growth. PeerJ 7:e7956 https://doi.org/10.7717/peerj.7956

Off-line and on-line optical monitoring of microalgal growth

Hugo-Enrique Lazcano-Hernandez [1], **Gabriela Aguilar** [2], **Gabriela Dzul** [2], **Rodrigo Patiño** [Corresp., 2], **Javier Arellano-Verdejo** [Corresp. 3]

[1] Cátedras CONACYT-El Colegio de la Frontera Sur, Chetumal, Quintana Roo, México

[2] Departamento de Física Aplicada, Cinvestav Unidad Mérida, Mérida, Yucatán, México

[3] Estación para la Recepción de Información Satelital ERIS-Chetumal, El Colegio de la Frontera Sur, Chetumal, Quintana Roo, México

Corresponding Authors: Rodrigo Patiño, Javier Arellano-Verdejo
Email address: rodrigo.patino@cinvestav.mx, javier.arellano@mail.ecosur.mx

The growth of *Chlamydomonas reinhardtii* microalgae cultures was successfully monitored, from classic off-line optical techniques (optical density and fluorescence) to on-line analysis of digital images. In this study, it is shown that the chlorophyll fluorescence ratio F_{685}/F_{740} has a linear correlation with the logarithmic concentration of microalgae. Moreover, with digital images, the biomass concentration was correlated with: the luminosity of the images through an exponential equation, and the length of penetration of a superluminescent blue beam (λ=440 nm), through an inversely proportional function. Outcomes of this study are useful to monitor both research and industrial microalgae cultures.

Off-line and on-line optical monitoring of microalgal growth

Hugo E. Lazcano-Hernandez[1], Gabriela Aguilar[2], Gabriela Dzul[2], Rodrigo Patiño[2], and Javier Arellano-Verdejo[3]

[1]**Catedras CONACYT-El Colegio de la Frontera Sur, Chetumal, Quintana Roo, México**
[2]**Cinvestav – Unidad Mérida, Departamento de Física Aplicada,A.P. 73, Cordemex, Mérida, Yucatán, México. C.P. 97310**
[3]**El Colegio de la Frontera Sur, Estación para la Recepción de Información Satelital ERIS-Chetumal, Av. Centenario Km 5.5 C.P. 77014, Chetumal, Quintana Roo, México. javier.arellano@mail.ecosur.mx**

Corresponding author:
Javier Arellano-Verdejo, Rodrigo Patiño

Email address: javier.arellano@mail.ecosur.mx, rodrigo.patino@cinvestav.mx

ABSTRACT

The growth of *Chlamydomonas reinhardtii* microalgae cultures was successfully monitored, from classic off-line optical techniques (optical density and fluorescence), to on-line analysis of digital images. In this study, it is shown that, the chlorophyll fluorescence ratio F_{685}/F_{740} has a linear correlation with logarithmic concentration of microalgae. Moreover, with digital images, the biomass concentration was correlated with: the luminosity of the images through an exponential equation, and the length of penetration of a super luminescent blue beam (λ=440 nm) through an inversely proportional function. Outcomes of this study are useful to monitor both research and industrial microalgae cultures.

INTRODUCTION

Photosynthesis is a biophotonic mechanism by which green plants, cyanobacteria and algae, transform a fraction of the solar energy, to produce their own food. This is the foundation of life on Earth. Photosynthesis occurs in the chloroplasts, which are those cell organelles that contain the photosynthetic pigments (chlorophyll a, chlorophyll b, carotenoids, etc.). They absorb light and use it to drive photosynthetic light reactions and associated electron transport reactions to reduce CO_2 and oxidize H_2O in the Calvin cycle (Allen, 1992). The net result of photosynthesis is the production of carbohydrates and the release of molecular oxygen to the atmosphere. Environmental factors such as temperature, irradiance, humidity and salinity are known to affect photosynthesis (Rym, 2012).

Currently, microalgae cultivation has been widely studied, due to the potential of microalgae as a source of food, biofuel and various bioactive compounds useful for important processes such as the cleaning of residual waters, CO_2 capture, and H_2 synthesis. All these are valuable products, which contributes to the balance and growth of human activity on a global scale (Gupta et al., 2015). Although there are several models of photobioreactors, in most cases the performance of measurements requires the extraction of samples by syringes or pipettes, which could pollute the culture, disturb algae physiological state, modify the volume of the medium, to mention only a few disadvantages. Another challenge for real-time measurements is the range increment in the concentration of microalgal cultures, which commonly increase of up to three times the original order of magnitude, which is out of range of most devices (Antal et al., 2019). Therefore, it is currently a challenge, to implement non-invasive real-time methodologies, for monitoring microalgal cultivation conditions and photosynthetic parameters (Antal et al., 2019).

Chlorophyll(*Chl*) molecules are organized into two groups of pigments, called Photosystem I (*PSI*) and Photosystem II (*PSII*), both spatially separated in thylakoid membranes of the chloroplasts (Breijo et al., 2006). Every photosystem contains an antenna light-harvestig complex (*LHC*) and central *Chl*

molecules. The photosystems differ from each other in their proportions of *Chl a* and *Chl b*, in the characteristics of the reaction centers, and in the electron carriers in their processes. In *PSI*, the reactive center is called *P700* and is formed by two *Chl a* molecules which are attached to each other. *PSII* also contains a reactive center called *P680*, formed also by two *Chl a* molecules. The nomenclature is associated with the maximum wavelength (λ) absorption of both *PSI* and *PSII*: λ=700 nm and λ=680 nm, respectively (Gouveia-Neto et al., 2011). According to the origin and kind of *Chl*, culture medium, the environmental conditions and the measurement equipment, the maximum fluorescence wavelength may vary. As an example, at room temperature, *Chl a* fluorescence around λ=685nm is largely emitted by *PSII* antenna, and fluorescence around λ=740 nm is emitted by *PSI* antenna (Krause and Weis, 1984; Roháček et al., 2008; Gouveia-Neto et al., 2011). In the fluorescence emission spectra of healthy dilute suspensions of thylakoid membranes or isolated chloroplasts, a sharp peak around λ=685 nm with a broad shoulder at about λ=740 nm is observed (Krause and Weis, 1991). Although isolated *Chl b* dissolved in organic solvent exhibits fluorescence, this does not happen with *in vivo* cultures, because the excitation energy is transferred completely to the *Chl a* (Gouveia-Neto et al., 2011).

The main function of the *LCH* is to transfer excitation energy to the photosynthetic reaction centers, where photochemical reactions take place; however, a part of absorbed light energy is dissipated as heat or emitted as fluorescence (Misra et al., 2012). In other words, to return to the ground state, the exited *Chl* molecule undergoes one of three fates: it can be (i) used to drive photochemical reactions (photosynthesis), (ii) dissipated as heat (thermal de-excitation), or (iii) re-emitted as light (fluorescence). These processes occur in competition, so that any increase in the efficiency of one will result in a decrease in the yield of the other two. *Chl* fluorescence represents an intrinsic signal emitted by plants, algae and cyanobacteria, which can be employed to monitor their physiological state, including changes in the photosynthetic apparatus, developmental processes, state of health, stress events, stress tolerance, and also to detect diseases or nutrient deficiency (Gouveia-Neto et al., 2011; Hák et al., 1990). Hence, by measuring the yield of *Chl* fluorescence, information about changes in the efficiency of photosynthesis and heat dissipation can be obtained (Maxwell and Johnson, 2000; Krause and Weis, 1984). Therefore, the simultaneous measuring of *Chl* fluorescence at λ=685 nm (F_{685}) and at λ=740 nm (F_{740}), allows for an approximate determination of *Chl* content in a non-destructive way, using the *Chl* ratio (F_{685}/F_{740}) (Hák et al., 1990).

Depending on the type of study and the suitability of the photosynthetic system, different fluorescence techniques have been used (Mauzerall, 1972; Olson et al., 1996; Kolber et al., 1998; Gorbunov and Falkowski, 2004; Johnson, 2004; Chekalyuk and Hafez, 2008). At present, *Chl* fluorescence approaches are used to monitor photosynthetic efficiency in microalgae mass cultures: rapid fluorescence induction and the saturation-pulse method (Masojídek et al., 2011), which are well known successful methods. Regarding outdoor algae cultures, specific fluorimeters have been used: pulse amplitude modulation (*PAM*) fluorimeter provides rapid light responses curves of *PSII*; otherwise, dual *PAM* fluorimeter estimate *PSI* and *PSII* yields and Induction Kinetics fluorimeter measure fluorescence induction curves (Sukenik et al., 2009; Kromkamp et al., 2009; Masojídek et al., 2010). However, real-time non-invasive methodologies are still needed to monitor the growth conditions of the microalgae culture. Therefore, two methodologies are proposed in this study, in order to measure the *Chlamydomonas reinhardtii* (*C. reinhardtii*) culture growth, through fluorescence measurements at room temperature: an analytic off-line optical technique and a on-line analysis of digital images. Microalga (*C. reinhardtii*), is considered one of the most promising eukaryotic H_2 producers (Torzillo et al., 2015), reason why its study is relevant. The methodologies proposed here were applied to study the growth of the *C. reinhardtii*, although it could be easily adapted to measure fluorescence in other photosynthetic microbial cultures.

1 MATERIALS AND METHODS

1.1 Microalgae cultures

The C. *reinhardtii* (CC-124) microalgae were purchased from the Chlamydomonas Resource Center (USA) and grown photoautotrophically in Sueoka medium (Sueoka, 1960). Growth conditions include continuous air bubbling ($1VVM = 1L-air/min/L-medium$) under controlled room temperature conditions (298 ± 2) K. Experiments were performed in two series: firstly for the off-line optical density and fluorimetry measurements (Experiments A and B), and then for the on-line techniques using digital images (Experiments 1 to 5). A portable spectrometer (*StellarNet, EPP2000*) was used to measure optical density, fluorescence and color of the microalgae cultures, with a detection range between 200 and 850

nm. The corresponding Spectrawiz software (StellarNet, OS V5.0 ©2011) was used for measurements with the spectrometer. In order to follow the cell growth, optical density (OD) measurements at $\lambda = 640$ nm were taken; each measurement was repeated three times for every sample. In a previous work, the dry weight of the microalgae was correlated with the OD of the algae cultures (del Campo et al., 2014).

For the off-line experiments, three $1-L$ Roux culture bottles were used, each with $0.9L$ of algae culture, with continuous air bubbling ($1L/min$), under controlled room temperature conditions ($298 \pm 2K$ (figure 1a). The cultures were illuminated continuously with two fluorescent lamps (Philips, $F20T12/D20W$). To assess the microalgae growth kinetics, every 12 hours during five days, three samples of $3mL$ each were taken from every bottle; additionally, a final control measurement was taken on the seventh day. OD and fluorescence measurements were taken for every sample. Two experiments were performed with the only difference for the initial microalgae concentration, x_0: Experiment $A, x_0 = (34 \pm 2)mg/L$, and Experiment $B, x_0 = (42 \pm 2)mg/L$.

For the on-line experiments, a $3-L$ column photo-bio-reactor (*PBR*) was used. A transparent acrylic tube with 25 mm of thickness and inner diameter of 95 mm, was used to build the $95-cm$ length *PBR*. Four fluorescent lamps (Tecno Lite, $T46500K20W$) were used to illuminate at the center of the column with around 100 μmol photons $m^{-2}s^{-1}$, avoiding external sources of light (figure 1b). Five experiments were performed, each during five days: three experiments with continuous illumination (Experiments 1, 2, and 3), and two experiments with 12-h light/12-h dark cycles (Experiments 4 and 5). Both off-line samples and digital images were taken every 6 or 12 h. A webcam (*Logitech, Carl Zeiss Tessar HD 1080 p*) connected to a PC was used to capture digital images of the PBR. For the color analysis, the images were captured with two fluorescent lamps turned on behind the *PBR* and the other two lamps turned off. For the fluorescent images, the pictures were captured in darkness and only illuminated with a blue beam from a super luminescent diode (maximal wavelength of 440 nm) and a light filter (*LSR-GARD ARGON, model 2204)* with a protection range in 190-520 nm. At least 15 min of darkness was assured before the fluorescent stimulation. The images were analyzed in a LCD screen with an Integrating cube (StellarNet, IC2) and the portable spectrometer. The International Commission on Illumination (CIELAB) scale was used for color measurements, and five measurements were taken from different regions for every image.

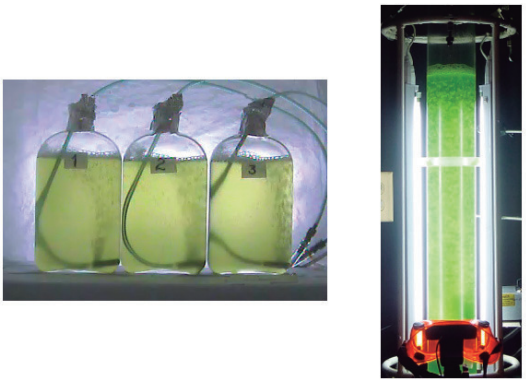

Figure 1. (a) The three Roux bottles for the off-line experiments (A and B), and (b) the column photo-bio-reactor (*PBR*) for the on-line experiments (1-5); see Materials and Methods

1.2 Fluorescence cabin

The experimental system to measure fluorescence is composed of two main parts: a fluorescence cabin and the portable spectrometer. Based on the spectrometer, the fluorescence cabin was designed, manufactured, and coupled to the system using an optical fiber (*StellarNet, F400*). Through this fiber, light was guided from the sample cuvette to the spectrometer detector. The fluorescence cabin configuration is shown in 2a. The main components are: a dark cabin, a cylindrical (14 mm i.d.) glass sample cuvette (4 mL), light emission diodes (LED), feed and switching electronic circuits, an AC/DC electric current converter (output 5.4 V) and a multi-modal optical fiber connector. The dark cabin is a space where light does not come in from external sources. Inside the dark cabin, a base was put to fix the cuvette in a normal position (at 90 degrees) relative to the floor. Parallel to the floor, as exciting radiation, six LEDs were placed

(Steren, Ultra Blue), three to the right side of the sample cuvette and three to the left. This configuration allows an homogeneous illumination. In 2b, a representative spectrum of the six LEDs is shown, with a maximum wavelength emission around λ=464 nm, luminosity of 7 cd and 400 mW as maximum power.

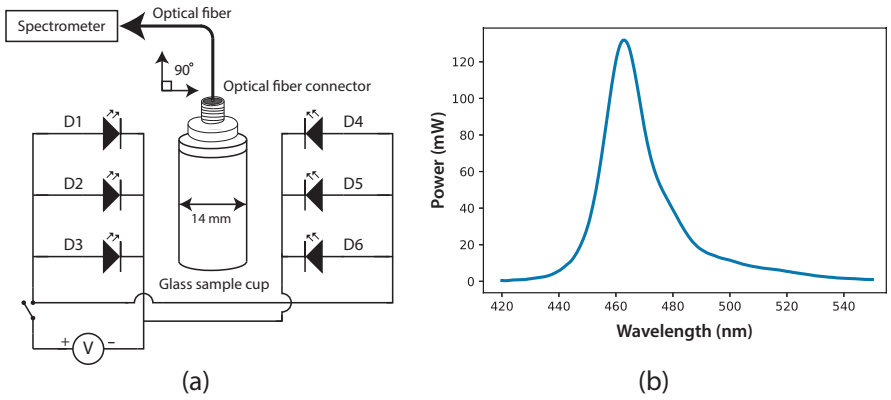

Figure 2. (a) Fluorescence cabin diagram, with optical fiber connector and glass sample cuvette; six Ultra Blue LEDs were installed as exciting source. (b) Spectrum of the exciting radiation source (Ultra Blue LEDs, λ max = 464 nm)

To improve the quality of the fluorescence measurements, the optical fiber was positioned on the top of the glass sample cuvette, at 90° relative to the LEDs radiation. Traditionally, fluorescence is measured through the sample cuvette wall. Instead of that, fluorescence measurements were taken on the uncovered top of the cuvette, thus achieving diminishing losses by reflection and refraction in the interface of the cuvette. The cuvette used for the samples was a 4-mL glass cylinder, but with this fluorescence system, the material and the geometry of the cuvette are not important. The light information is processed and digitalized by the spectrometer SpectraWiz software. To start measurements, zero level must be defined, setting the spectrometer with Sueoka medium; then, the fluorescence measurement is performed on the microalgae sample. Direct fluorescence of *C. reinhardtii* culture samples, at room temperature, were successfully measured throughout seven days with this experimental setup. The ratio of fluorescence intensity between λ=685 and λ=740 nm was calculated.

1.3 The F_{685}/F_{740} fluorescence ratio

At low *Chl* concentrations, fluorescence emissions increase with increasing quantity of *Chl*. At higher concentrations, the increase of fluorescence with the increment of *Chl* is mainly detected around 740 nm. For in vivo cultures, fluorescence emission at 740 nm is favored (and fluorescence emission at 685 nm is not favored), because of (i) the re-absorption of photons from the fluorescence emitted by neighboring molecules, (ii) the light interference between the short (685 nm) and long wavelengths (740 nm), and (iii) the increment of *Chl* (the new *Chl* molecules preferentially absorb energy at 685 nm) (Gouveia-Neto et al., 2011).

There is a good inverse correlation between photochemistry and *Chl* fluorescence. The ratio of fluorescence intensity between maxima wavelengths (F_{685}/F_{740}) is influenced by the photosynthetic activity. In mature microalgae cultures, the chloroplast structure, CO_2 uptake rate, carbon metabolism, etc., are better than in the younger cells. Higher F_{685}/F_{740} values, indicate young cultures or cultures with photosynthetic apparatus not yet fully developed. Low values indicate mature cultures with a fully developed photosynthetic apparatus. In other words, the decrement in F_{685}/F_{740} value is indicative of increased photosynthetic activity. Measured through induction fluorescence, F_{685}/F_{740} exhibits a curvilinear relationship with the cells concentration, x, which can be successfully expressed by equation 1, where c and d are constants (Hák et al., 1990):

$$\frac{F_{685}}{F_{740}} = cx^{-d} \tag{1}$$

This technique has been applicable to all kinds of leaves, chloroplast suspensions and acetone extracts

PeerJ Preprints | https://doi.org/10.7287/peerj.preprints.27744v1 | CC BY 4.0 Open Access | rec: 19 May 2019, publ: 19 May 2019

of photosynthetic pigments. In this work, it is demonstrated that this technique is also applicable to microalgae cultures.

2 RESULTS AND DISCUSSION

2.1 Microbial growth

It has been established in a previous work that the Gompertz model represents the *C. reinhardtii* growth better than the classical Monod model (del Campo et al., 2014). Actually, the Monod and Gompertz models can be seen as particular cases of a more universal growth model (Castorina et al., 2006). For the experiments in the Roux bottles (A and B), as well as in the *PBR* (1-5), the Gompertz specific growth rate is reported in table 1. For the *PBR* experiments, it is possible to observe that Gompertz model is best fitted when the light regime is continuous (see R^2 for experiments 1-3) than when light/dark cycles are performed (experiments 4-5). Moreover, the specific growth rate is favored when the *PBR* is used, in contrast with the cultures in the Roux bottles.

Reactor	Experiments	$\mu(day^{-1})$	R^2
Roux bottles	AI	0.5472	0.9981
	AII	0.5856	0.9989
	AIII	0.5424	0.9889
		0.56 ± 0.02	
	BI	0.3360	0.9843
	BII	0.4032	0.9965
	BIII	0.3696	0.9944
		0.37 ± 0.03	
PBR	1	0.7824	0.9954
	2	0.6720	0.9771
	3	0.6192	0.9656
		0.69 ± 0.08	
	4	0.3384	0.9180
	5	0.4776	0.9312
		0.41 ± 0.10	

Table 1. The Gompertz specific growth rate of microalgae in seven experiments, with the corresponding correlation values. The mean value and the standard deviation are reported for the cultures with continuous illumination (experiments A and B in the Roux bottles, and 1, 2, and 3 in the PBR) and with light/dark cycles (experiments 4 and 5 in the PBR).

2.2 Fluorescence measurements

The variations in fluorescence intensity were successfully measured, according to the increment in the *C. reinhardtii* concentration. Some selected spectra are shown in Figure 3 for experiment A. Fluorescence Dataset for experiments A and B are shown in suplementary material file (S1). In all cases, *Chl* fluorescence exhibits a peak around λ=685 nm and a broad shoulder around λ=740 nm; this is a general observation at room temperature for *Chl a* (Gouveia-Neto et al., 2011; Krause and Weis, 1984). The fluorescence around λ=685 nm is attributed to the *PSII* antenna, and the fluorescence around λ=740 nm is due to the PSI antenna (Gouveia-Neto et al., 2011). The fluorescence signal/noise ratio in our measurements was around 7 at λ=740 nm and 14 at λ=685 nm.

In Figure 4, the fluorescence evolution at λ=685 nm and at λ=740 nm is shown for all bottles of experiments A. The plots include trend lines. In both experiments A and B, the maximum fluorescence intensity at λ=685 nm occurs between 48 and 60 hours: after that time, fluorescence decreases. Regarding fluorescence at λ=740 nm, in Experiment A, the maximum value occurred at 72 hours in all cultures; and in Experiment B, the maximum value happened between 96 and 108 hours. For both experiments, the maximum fluorescence at λ=685 nm occurs before than at λ=740 nm; and maximum fluorescence at λ=740 nm occurs at the highest concentrations of algae. In general, the results are consistent with those described in the literature for fluorescence in plants (Gouveia-Neto et al., 2011). Namely, at low

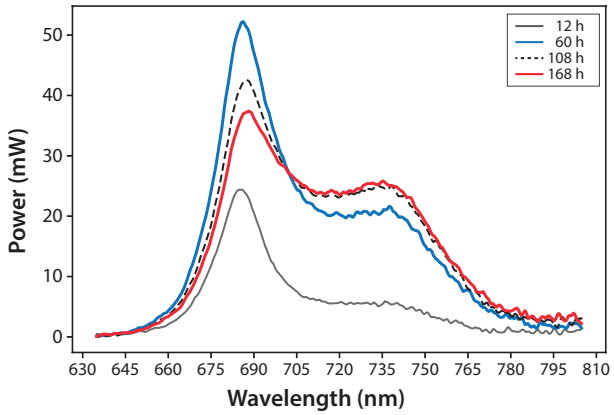

Figure 3. Microalgae fluorescence emission spectra ($298 \pm 2K$): evolution throughout seven days (168 h). Experiment $A, x_0 = (34 \pm 2)$ mg/L

Chl concentrations, the fluorescence emissions increase with increasing *Chl* concentration. At higher concentrations, the increase of fluorescence with the increment of *Chl* was detected only around λ=740 nm.

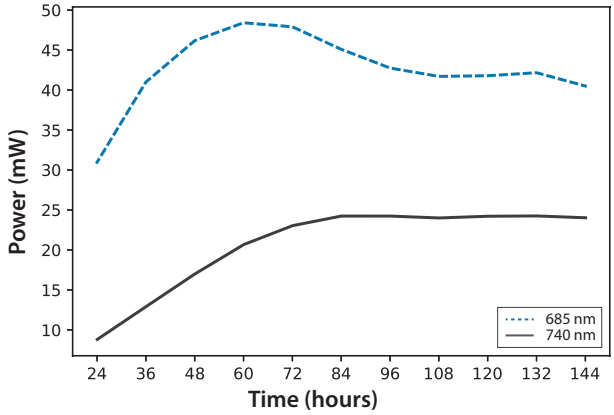

Figure 4. Experiment A:*C. reinhardtii* Fluorescence evolution trend at $\lambda = 685$ nm and $\lambda = 740$ nm

Regarding the F_{685}/F_{740} ratio, it is possible to observe a similar behavior in every culture of both experiments, regardless of the initial concentration. For that reason, in Figure 5 it is shown the average of the three cultures for each of the two experiments, over five days and a final measurement on the seventh day. As time went by, the F_{685}/F_{740} fluorescence ratio decreased, and that means that the photosynthetic processes were improved. The same trend has been reported for green leaves in plants, as stated in equation 1 (Hák et al., 1990).

Based on information in Figure 5, and considering the data from 168 hours as the minimum possible (aged crops), we figured that cultures in both experiments reached around 70% of maturity at 96 hours. Therefore, every culture is evolving successfully, which means that the conditions are appropriate to grow the microalgae and keep them in a good state of health. In addition, the cultures that reached the lowest F_{685}/F_{740} values, that is, the highest photosynthetic activity, were those of Experiment A, which were started with the lowest initial concentration. Moreover, after 72 hours, these values did not change significantly and this is the moment when illumination may not be enough for the culture because the concentration of cells reduces the path of light. Finally, a very useful linear correlation occurs for the logarithmic concentration of microalgae and the F_{685}/F_{740} ratio through time (Figure 6):

$$ln\left(\frac{x}{x_0}\right) = 3.27 - 0.7084(F_{685}/F_{740}) \quad (2)$$

PeerJ Preprints | https://doi.org/10.7287/peerj.preprints.27744v1 | CC BY 4.0 Open Access | rec: 19 May 2019, publ: 19 May 2019

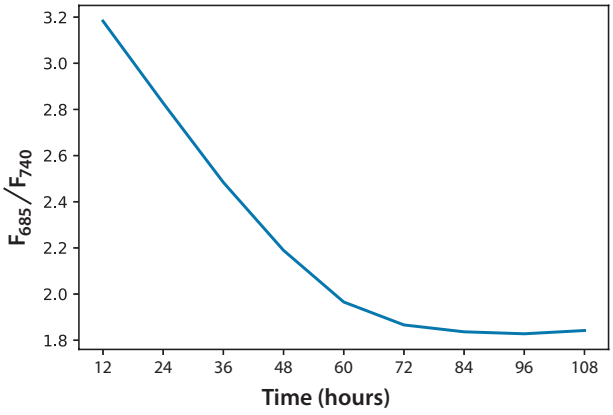

Figure 5. Fluorescence ratio (F_{685}/F_{740}) trend for *C. reinhardtii*

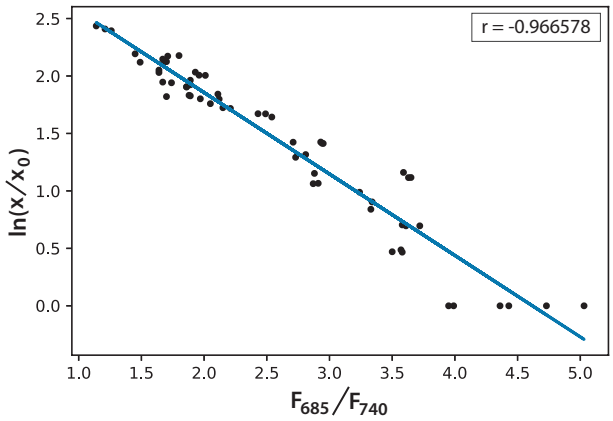

Figure 6. Linear correlation for the logarithmic microalgae concentration and the fluorescence ratio $F_{685}/F_{740}(r = -0.966578)$

2.3 Digital images

When the *PBR* was used, digital images of the cultures were taken to follow the change in color and to measure the penetration of a fluorescent beam during the microalgae growth. A selection of images is presented in Figure 7 for a typical experiment. It is possible to observe that cultures get darker with time due to the increase of biomass concentration in the *PBR*, which avoid the pass of light throughout the reactor. For the fluorescence measurements, the flashes due to the blue super-luminescent diode were filtered in order to measure only the fluorescence ligth contribution, which diminishes with time due to a shadow effect by cells when the microalgae concentration gets denser.

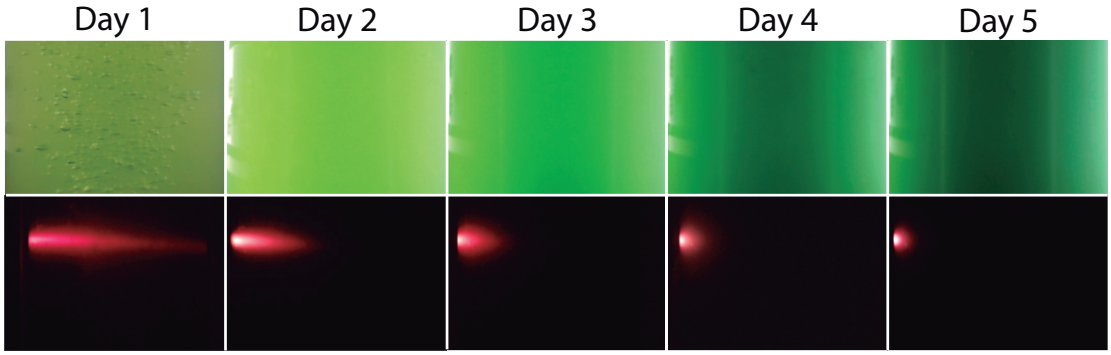

Figure 7. Representative images of the *PBR* captured every day during an experiment

PeerJ Preprints | https://doi.org/10.7287/peerj.preprints.27744v1 | CC BY 4.0 Open Access | rec: 19 May 2019, publ: 19 May 2019

CIELAB measurements include three values to characterize the color of a sample: L is the luminosity, the parameter "a" for colors from green to red, and the parameter "b" for colors from blue to yellow. Both "a" and "b" parameters, rest almost constant along the time of the experiment during microalgae growth. This means that, technically, color does not change, which is expected since the photosynthetic pigments are always the same. In fact, luminosity is what diminishes importantly during cell growth, since cells deviate or shadow light sources. In Figure 8, it is possible to observe the logarithmic correlation between the microalgae concentration x, and the luminosity L for experiments 1-3. For these experiments, the equation 3 is proposed to get x from on-line measurements of L from digital images:

$$ln\left(\frac{x}{x_0}\right) = (1.6 \pm 0.2) - (0.44 \pm 0.04)(L/W) \tag{3}$$

In this equation, the intercept and the slope values are presented as the mean and the corresponding standard deviation from the individual correlations in the three experiments (see Figure 8). However, this same correlation was not observed in experiments 4-5, where light/dark cycles were performed (data not shown). Calculation of the correlations between the values of the three experiments confirms that the experiments are reproducible, which gives confidence to the study. Table 2 shown $L(W)$ values correlation and Table 3 shown correlation between $ln(x/x_0)$ values.

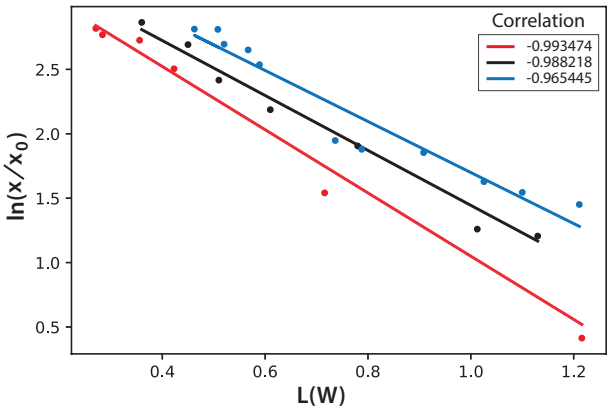

Figure 8. Logarithmic dependence of cell concentration with the luminosity (L) value in the CIELAB scale of colors, for the PBR experiments with continuous illumination. The colors correspond to experimental values: black (experiment 1), red (experiment 2), and blue (experiment 3); the lines correspond to the mean-squares correlations

	E1	E2	E3
E1	1.000000	0.963332	0.942350
E2	0.963332	1.000000	0.973427
E3	0.942350	0.973427	1.000000

Table 2. $L(W)$ Correlation

	E1	E2	E3
E1	1.000000	0.973283	0.948333
E2	0.973283	1.000000	0.985426
E3	0.948333	0.985426	1.000000

Table 3. $ln(x/x_0)$ Correlation

Finally, the fluorescence beam penetration was characterized as an image changing with time: both surface area of the beam (data not shown) and the distance of the beam penetration, were used to follow

PeerJ Preprints | https://doi.org/10.7287/peerj.preprints.27744v1 | CC BY 4.0 Open Access | rec: 19 May 2019, publ: 19 May 2019

these changes. Similar results were obtained when comparing the cell concentration with the changes in the fluorescent images; therefore, only the distance beam penetration was used since its measurement is much simpler than the surface area. In Figure 9, it is possible to observe the correlation of this distance measured for the fluorescent beam penetration with the inverse of the OD. As stated before, the OD is already related with the biomass concentration (Martín del Campo, 2014). It is important to notice that the linear correlations were obtained for all 1-5 experiments, with the equation 4 proposed to calculate the OD of the culture directly from the on-line measure of the beam penetration:

$$OD = \frac{1}{\text{beam penetration / cm}} \tag{4}$$

This simple equation is proposed since the values for the mean and the corresponding standard deviation for the intercept and the slope in the individual linear correlations for the five experiments are, respectively, (0.0 ± 0.5) and $(1.0 \pm 0.1) cm^{-1}$.

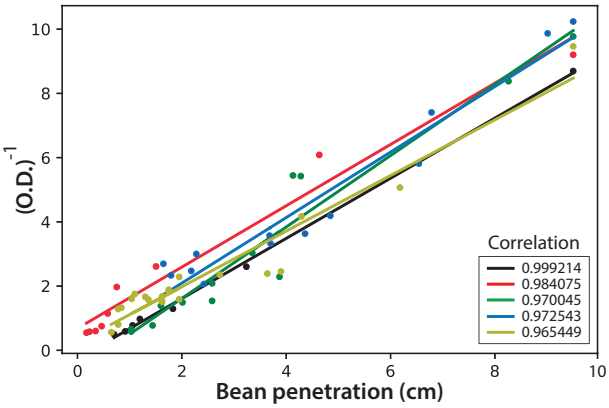

Figure 9. The inverse of the optical density (OD) for the microalgae cultures, as a function of the fluorescent beam penetration in the PBR. The colors correspond to the experimental values: black (experiment 1), red (experiment 2), green (experiment 3), blue (experiment 4) and light green (experiment 5); the lines correspond to the least-squares correlations.

3 CONCLUSIONS

Growth of *C. reinhardtii* cultures were successfully monitored throughout off-line and on-line optical techniques at affordable cost. It was confirmed that, as evidenced in green plants, the maximum fluorescence around λ=685 nm occurs before than that happening at λ=740 nm. The maximum fluorescence at λ=740 nm occurs at a higher concentration, compared to what is needed at λ=685 nm. Once the maximum fluorescence at λ=685 nm has been reached, its decrement occurs before and at a faster rate that the fluorescence at λ=740 nm. Although the F_{685}/F_{740} fluorescence ratio is a method that has been well known, here is demonstrated for *C. reinhardtii* cultures. A very useful linear correlation occurs between logarithmic concentration of *C. reinhardtii* and the F_{685}/F_{740} ratio through time.

Moreover, the on-line analysis of digital images was shown to be also useful to track the *C. reinhardtii* growth. The luminosity measurements in the CIELAB scale were linearly correlated with the microbial concentration for cultures under continuous illuminations; however, for the cultures in a light/dark regime, this correlation was not found. Nevertheless, for the fluorescent beam penetration images, both the distance and the surface captured for the beam, were linearly correlated with the optical density and, consequently, with the microalgae culture density for all the illumination regimes. Indeed, a simple reciprocal equation can be used to calculate the optical density as the inverse of the measured distance of the beam penetration.

The on-line techniques proposed here, are very practical to study both research and industrial microalgae cultures, including remote sensing applications.

ACKNOWLEDGMENTS

Hugo Lazcano thanks CONACyT for his postdoctoral fellowship and for the support provided through the "Cátedras" for young Investigators program (project 526).

FUNDING

This research did not receive any specific grant from funding agencies in the public, commercial, or not-for-profit sectors.

REFERENCES

Allen, J. F. (1992). How does protein phosphorylation regulate photosynthesis? *Trends in biochemical sciences*, 17(1):12–17.

Antal, T., Konyukhov, I., Volgusheva, A., Plyusnina, T., Khruschev, S., Kukarskikh, G., Goryachev, S., and Rubin, A. (2019). Chlorophyll fluorescence induction and relaxation system for the continuous monitoring of photosynthetic capacity in photobioreactors. *Physiologia plantarum*, 165(3):476–486.

Breijo, F. J. G., Caselles, J. R., and Siurana, P. S. (2006). *Introducción al funcionamiento de las plantas*. Ed. Univ. Politéc. Valencia.

Castorina, P., Delsanto, P., and Guiot, C. (2006). Classification scheme for phenomenological universalities in growth problems in physics and other sciences. *Physical review letters*, 96(18):188701.

Chekalyuk, A. and Hafez, M. (2008). Advanced laser fluorometry of natural aquatic environments. *Limnology and Oceanography: Methods*, 6(11):591–609.

del Campo, J. S. M., Escalante, R., Robledo, D., and Patino, R. (2014). Hydrogen production by chlamydomonas reinhardtii under light-driven and sulfur-deprived conditions: using biomass grown in outdoor photobioreactors at the yucatan peninsula. *international journal of hydrogen energy*, 39(36):20950–20957.

Gorbunov, M. Y. and Falkowski, P. G. (2004). Fluorescence induction and relaxation (fire) technique and instrumentation for monitoring photosynthetic processes and primary production in aquatic ecosystems. In *Photosynthesis: Fundamental Aspects to Global Perspectives"-Proc. 13th International Congress of Photosynthesis, Montreal, Aug*, pages 1029–1031.

Gouveia-Neto, A. S., da Silva-Jr, E. A., Cunha, P. C., Oliveira-Filho, R. A., Silva, L. M., da Costa, E. B., Camara, T. J., and Willadino, L. G. (2011). Abiotic stress diagnosis via laser induced chlorophyll fluorescence analysis in plants for biofuel. In *Biofuel Production-Recent Developments and Prospects*. IntechOpen.

Gupta, P. L., Lee, S.-M., and Choi, H.-J. (2015). A mini review: photobioreactors for large scale algal cultivation. *World Journal of Microbiology and Biotechnology*, 31(9):1409–1417.

Hák, R., Lichtenthaler, H., and Rinderle, U. (1990). Decrease of the chlorophyll fluorescence ratio f690/f730 during greening and development of leaves. *Radiation and environmental biophysics*, 29(4):329–336.

Johnson, Z. I. (2004). Description and application of the background irradiance gradient-single turnover fluorometer (big-stf). *Marine Ecology Progress Series*, 283:73–80.

Kolber, Z. S., Prášil, O., and Falkowski, P. G. (1998). Measurements of variable chlorophyll fluorescence using fast repetition rate techniques: defining methodology and experimental protocols. *Biochimica et Biophysica Acta (BBA)-Bioenergetics*, 1367(1-3):88–106.

Krause, G. and Weis, E. (1991). Chlorophyll fluorescence and photosynthesis: the basics. *Annual review of plant biology*, 42(1):313–349.

Krause, G. H. and Weis, E. (1984). Chlorophyll fluorescence as a tool in plant physiology. *Photosynthesis research*, 5(2):139–157.

Kromkamp, J. C., Beardall, J., Sukenik, A., Kopeckỳ, J., Masojídek, J., Van Bergeijk, S., Gabai, S., Shaham, E., and Yamshon, A. (2009). Short-term variations in photosynthetic parameters of nannochloropsis cultures grown in two types of outdoor mass cultivation systems. *Aquatic Microbial Ecology*, 56(2-3):309–322.

Masojídek, J., Kopeckỳ, J., Giannelli, L., and Torzillo, G. (2011). Productivity correlated to photobiochemical performance of chlorella mass cultures grown outdoors in thin-layer cascades. *Journal of industrial microbiology & biotechnology*, 38(2):307–317.

Masojídek, J., Vonshak, A., and Torzillo, G. (2010). Chlorophyll fluorescence applications in microalgal mass cultures. In *Chlorophyll a fluorescence in aquatic sciences: methods and applications*, pages 277–292. Springer.

Mauzerall, D. (1972). Light-induced fluorescence changes in chlorella, and the primary photoreactions for the production of oxygen. *Proceedings of the National Academy of Sciences*, 69(6):1358–1362.

Maxwell, K. and Johnson, G. N. (2000). Chlorophyll fluorescence—a practical guide. *Journal of experimental botany*, 51(345):659–668.

Misra, A. N., Misra, M., and Singh, R. (2012). Chlorophyll fluorescence in plant biology. In *Biophysics*. IntechOpen.

Olson, R. J., Chekalyuk, A. M., and Sosik, H. M. (1996). Phytoplankton photosynethetic characteristics from fluorescence induction assays of individual cells. *Limnology and oceanography*, 41(6):1253–1263.

Roháček, K., Soukupová, J., Barták, M., et al. (2008). Chlorophyll fluorescence: a wonderful tool to study plant physiology and plant stress. *Plant Cell Compartments-Selected Topics. Research Signpost, Kerala, India*, pages 41–104.

Rym, B. D. (2012). Photosynthetic behavior of microalgae in response to environmental factors. In *Applied Photosynthesis*. IntechOpen.

Sueoka, N. (1960). Mitotic replication of deoxyribonucleic acid in chlamydomonas reinhardi. *Proceedings of the National Academy of Sciences of the United States of America*, 46(1):83.

Sukenik, A., Beardall, J., Kromkamp, J. C., Kopeckỳ, J., Masojídek, J., van Bergeijk, S., Gabai, S., Shaham, E., and Yamshon, A. (2009). Photosynthetic performance of outdoor nannochloropsis mass cultures under a wide range of environmental conditions. *Aquatic Microbial Ecology*, 56(2-3):297–308.

Torzillo, G., Scoma, A., Faraloni, C., and Giannelli, L. (2015). Advances in the biotechnology of hydrogen production with the microalga chlamydomonas reinhardtii. *Critical reviews in biotechnology*, 35(4):485–496.

PeerJ Preprints | https://doi.org/10.7287/peerj.preprints.27744v1 | CC BY 4.0 Open Access | rec: 19 May 2019, publ: 19 May 2019